

# Effective medium approach in the renormalization group theory of phase transitions

V I Tokar

*Université de Strasbourg, CNRS, IPCMS, UMR 7504, F-67000 Strasbourg, France*

---

## Abstract

An effective medium approach similar to the coherent potential approximation (CPA) in the theory of disordered alloys and to the DMFT has been extended to the renormalization group equations in the local potential approximation (LPA). Non-universal characteristics of the second order phase transitions such as the critical temperatures and critical amplitudes have been calculated in good agreement with the best known estimates. A possibility of cluster extension of the LPA to improve its accuracy and to make the approach systematic and self-contained has been discussed. A qualitative explanation of the discrepancy between theoretical value of the critical exponent  $\beta$  and recent experimental data on ordering in beta brass by the influence of non-universal contributions has been suggested.

*Keywords:* self-consistent renormalization group equation, layer-cake renormalization scheme,  $n$ -vector spin models, critical temperatures, critical amplitudes, ordering in beta brass

---

## 1. Introduction

Phase transitions in many-body systems can be formally defined as the points where the free energy is singular with respect to the parameters entering the partition function, such as the external field and the temperature. Because microscopic Hamiltonians depend analytically on the parameters, the calculations of the free energy by a finite order series expansion in powers of the Hamiltonian or of its part cannot be singular. This means that phase transitions can be described only within non-perturbative approaches capable of calculating the free energy to all orders in the Hamiltonian which in general is a difficult task.

The problem simplifies in lattice models where the infinite system can be modeled by a finite cluster of lattice sites. In classical models which will be discussed in the present Letter the cluster partition function can be calculated exactly to all orders in Hamiltonian and with a suitable embedding of the cluster

---

*URL:* [tokar@ipcms.unistra.fr](mailto:tokar@ipcms.unistra.fr) (V I Tokar)

into the infinite system remarkably accurate results can be obtained with the use of small clusters [1, 2, 3, 4]. The cluster approximation is systematic in the sense that it can be indefinitely improved by enlarging the cluster size, so in principle it presents a viable alternative to the series expansions as a general approach to many-body problems with strong interactions. The main drawback of the cluster approach is that computationally accessible dimensions of the clusters are limited so it is impossible to adequately treat very long-range correlations [2, 4] which are indispensable in the description of the second order phase transitions and critical phenomena [5].

The critical behavior can be effectively described within the renormalization group (RG) theory [5, 6] which proved to be efficient in the vicinity of critical points where interactions between large-scale fluctuations weaken and sophisticated perturbative techniques make possible precision calculations of the universal quantities, such as the critical exponents and the critical amplitudes ratios [7, 8]. Experimentally, however, mainly non-universal quantities are measured, such as the critical temperatures and individual critical amplitudes, but their theoretical calculation in strongly coupled cases meets with difficulties. Current non-perturbative RG approaches [9, 6, 10, 8] suffer from poorly controlled approximations and so are not reliable enough to quantitatively predict non-universal quantities. Presumably because of this, phenomenological theories and the high-temperature expansions of simple model systems developed before the advent of the RG theory are still being invoked to interpret experimental data on the second-order phase transitions (see [11] and references therein).

Taking into account that some non-universal quantities, such as the critical temperatures, can be calculated with good accuracy within the cluster method [2, 4], in the spirit of the RG approach it would be natural to use some cluster technique to account for the short-range fluctuations and resort to RG only for the treatment of the long-range ones. A step in realization of this approach was made in [10] where the authors have succeeded in calculating a magnetization curve and several critical temperatures in good agreement with the best known values. This, however, was achieved with the introduction of arbitrary parameters into the calculations which casts doubts on the predictive abilities of the approach. Besides, no recipe was given of incorporation into the RG procedure of the notion of the effective medium which is central in the existing cluster approaches [2, 3, 4] was not introduced in the in the RG scheme in [10].

However, sound though not rigorous arguments exist that it is the self-consistency equations defining the effective medium underlie the success of such renowned methods as the coherent potential approximation (CPA) and the dynamical mean-field theory (DMFT) in the strong coupling regime (see the bibliography to the subject in review articles [12, 3] and also [13, 14]). Especially relevant to us is the CPA because by means of the replica trick the disordered alloy model can be reduced to a particular case ( $n = 0$ ) of the  $n$ -vector models which are the subject of the present study.

The main aim of this Letter is to derive a renormalization scheme based on the local potential approximation (LPA) [15, 16] and a self-consistency condi-

tion for the effective medium [13] formally the same as was used in the cluster approach in [2, 4], though currently based only on the single-site cluster so the scheme will be analogous to the single-site approximations (SSA) such as CPA and DMFT. It will be shown that the implementation of the self-consistent LPA scheme (SC-LPA) makes possible accurate calculation of non-universal quantities without use of arbitrary parameters. As a first physical application of the method, semi-quantitative arguments will be presented that the non-universal contributions may be responsible for the discrepancy between the universal value of the critical exponent  $\beta$  calculated within RG theory and the values obtained in recent experiments on ordering in beta-brass [11].

## 2. Definitions and notation

In this Letter we will deal with classical statistics of the  $n$ -vector models which describe real continuous  $n$ -component lattice fields on periodic  $d$ -dimensional lattices which interactions are described by Hamiltonians of the following general form

$$H[\mathbf{s}] = \frac{1}{2} s_{\sigma i} \epsilon_{ij} s_{\sigma j} + \sum_i H_I(\mathbf{s}_i) = \frac{1}{2} s_{\sigma} \hat{\epsilon} s_{\sigma} + H_I[\mathbf{s}]. \quad (1)$$

Here the first terms on the right hand side (r.h.s.) describes the pair interaction between the fields  $s_{\sigma} = \{s_{\sigma i}\}$  at sites  $i$  and  $j$  which may be different while the interaction part  $H_I$  is assumed to be local to the sites. Small Latin subscripts denote integer  $d$ -dimensional site coordinates, the Greek subscripts  $\sigma = 1, \dots, n$  refer to the  $n$ -vector components. The boldface quantities will denote the  $n$ -vectors and also the  $d$ -dimensional momenta  $\mathbf{k}_m$  in the lattice Fourier transform over spatial coordinates, but the integer  $d$ -dimensional lattice site vectors  $i, j$  for simplicity will not be boldfaced. To farther simplify notation, summation over repeated discrete (but not continuous) subscripts will be implicitly assumed throughout the paper. Besides, vector-matrix notation for the lattice coordinates will be used as, e.g., in the matrix of the pair couplings  $\hat{\epsilon} = \|\epsilon_{ij}\|$  in (1). In the general anisotropic case the couplings may depend also on  $\sigma$  but in the present paper only fully  $O(n)$ -symmetric Hamiltonians will be considered.

It is important to note that separation of  $H$  into the quadratic and the interaction parts in (1) is not unique because an arbitrary quadratic term can be added to the first part and simultaneously subtracted from  $H_I$  with the total Hamiltonian remaining unchanged. This trick will be essential in the effective medium theory in the next section but in (1) it will be used only to impose on  $\epsilon_{ij}$  the requirement that its Fourier transform behaved at small  $\mathbf{k}$  as

$$\epsilon(\mathbf{k})|_{\mathbf{k} \rightarrow 0} \propto \mathbf{k}^2 \quad (2)$$

which is convenient in implementation of the RG technique [5].

The partition function of the  $n$ -vector models is defined by the multiple integral over  $N$  values  $\{\mathbf{s}_i\}$  ( $N$  the number of lattice sites) of field  $\mathbf{s}$  as

$$Z[\mathbf{h}] = \int \prod_i d\mathbf{s}_i e^{-H[\mathbf{s}] + \mathbf{h}_i \cdot \mathbf{s}_i} \quad (3)$$

where the source field  $\mathbf{h}$  has been introduced so that the partition function can be used as the generating functional of the correlation functions (CFs) of the field.

By the linked cluster theorem the generating functional of connected CFs is given by  $\ln Z[\mathbf{h}]$ . Two such CFs will be needed in the present study: the magnetization

$$m_{\sigma i} \equiv \langle s_{\sigma i} \rangle = \left. \frac{\partial \ln Z[\mathbf{h}]}{\partial h_{\sigma i}} \right|_{\mathbf{h}=\mathbf{0}}, \quad (4)$$

and the connected part of the pair CF  $G_{ij}^R$

$$G_{ij}^R = \left. \frac{\partial^2 \ln Z[\mathbf{h}]}{\partial h_{\sigma i} \partial h_{\sigma j}} \right|_{\mathbf{h}=\mathbf{0}} = \langle s_{\sigma i} s_{\sigma j} \rangle - m_{\sigma i} m_{\sigma j}. \quad (5)$$

Though in general case non-trivial pair correlations between all field components may exist, the CFs diagonal in  $\sigma$  defined in (5) are sufficient in the fully  $O(n)$  symmetric case that will be considered in the present paper in the  $n > 1$  models. All diagonal CFs are equal due to the symmetry so the subscript  $\sigma$  may be dropped. The spontaneous symmetry breaking will be discussed only for the Ising model with  $n = 1$  so the subscript would be also superfluous. In (5) and throughout the paper superscript  $R$  denotes fully renormalized quantities.

The Fourier transformed CF (5) may be expressed through the exact mass (or self-energy) operator  $r^R$  as

$$G^R(\mathbf{k}) = \frac{1}{\epsilon(\mathbf{k}) + r^R(\mathbf{k})}. \quad (6)$$

This representation is convenient in approximate calculations because unlike  $G^R$  which in the vicinity of the critical point  $r^R(\mathbf{k} \rightarrow 0) \rightarrow 0$  is strongly momentum-dependent (see (2)), the mass operator in many cases can be approximated by a momentum-independent constant as, for example, in the CPA, in DMFT, and in the critical region [5].

### 3. Functional-differential formalism and the self-consistency condition

A general self-consistency equation for the mass operator within the functional formalism is discussed in detail in [13, 2, 4, 17] so below only short explanations will be given to the formulas that will be needed in subsequent calculations.

In strongly coupled models the calculation of the exact  $r^R(\mathbf{k})$  is usually beyond the reach so one has to resort to approximate treatments. Useful approximations adopted, e.g., in CPA and DMFT, can be obtained by the neglect of the momentum dependence of the self-energy. In the case under consideration this amounts to assuming that the exact  $G^R$  (6) can be approximated by the following trial CF

$$G(\mathbf{k}) = \frac{1}{\epsilon(\mathbf{k}) + r} \approx G^R(\mathbf{k}). \quad (7)$$

The last equality means that the momentum-dependent function  $r^R(\mathbf{k})$  is approximated by  $\mathbf{k}$ -independent constant  $r$ . Obviously, there is much ambiguity in doing this which can be used to adjust the approximation to satisfy some condition. In the SSA, like CPA and DMFT,  $r$  is set to be the average  $r \approx N^{-1} \sum_{\mathbf{k}} r^R(\mathbf{k})$  over the Brillouin zone (BZ) which is equivalent to assuming that the mass operator is diagonal in the lattice coordinates. From the  $\mathbf{k}$ -space standpoint this means that all Fourier momenta are equally important in the problem under consideration.

But in the critical region the most important are not local contributions but those with the largest spatial extent, i.e., with the smallest  $\mathbf{k}$ , so it seems natural to account for this by setting

$$r \approx r^R(\mathbf{k} = 0). \quad (8)$$

The adequacy of this approximation will be verified in explicit calculations below but it can be immediately noted that  $G^R \approx G$  presupposes that the critical exponent  $\eta = 0$  because at the critical point  $r = 0$  and from (2) it follows that as  $|\mathbf{k}| \rightarrow 0$   $G \sim 1/\mathbf{k}^2$ . This deficiency makes the approximation poorly suited for 2D systems where  $\eta$  has an appreciable value so only 3D models will be treated in the explicit calculations in section 5.

Explicit self-consistency condition for  $r$  similar to the CPA and DMFT equations is obtained as follows. First, the field-dependent partition function (3) which is the generating functional of CFs can be expressed through the generating functional of the scattering matrix  $S$  as [18, 19]

$$Z[\mathbf{h}] = e^{\frac{1}{2}h_\sigma \hat{G} h_\sigma} S[\mathbf{h}\hat{G}] \quad (9)$$

or, equivalently,

$$\ln Z[\mathbf{h}] = \frac{1}{2}h_\sigma \hat{G} h_\sigma - U^R[\mathbf{h}\hat{G}] \quad (10)$$

where  $U^R$  is the generating functional of the connected part of  $S$  and CF  $G$  defined in (7) fulfills the role of the propagator. Here and below the terminology from the quantum field theory, such as the scattering matrix, the propagator, etc., has been used which may not have much physical meaning in statistical models but the formalism we are using is universal [19] and the use of the established terminology should facilitate comparison with physically different but formally similar theories, such as the CPA and DMFT.

$$U^R = \textcircled{u_0^R} + \frac{1}{2} \textcircled{u_2^R} + \frac{1}{4!} \textcircled{u_4^R} + \dots$$

Figure 1: Tree terms of expansion of  $U^R[\phi]$  in powers of  $\phi$  for the functional even in the field variable.

The validity of expressions (9) and (10) is easy to understand diagrammatically. The connected diagrams for S-matrix (see figure 1) differ from the diagrams for  $\ln Z$  in that they describe either (quasi)particle scattering or reactions but not the free propagation. This is accounted for by the first term on the r.h.s. of (10). Another distinction is that the diagrams in the generating functional of S-matrix [13, 2, 4, 17]

$$S[\phi] = \det(2\pi\hat{G})^{n/2} \exp\left(\frac{1}{2}\partial_{\phi_\sigma}\hat{G}\partial_{\phi_\sigma}\right) e^{\frac{r}{2}\phi_i\cdot\phi_i - H_I[\phi]} \quad (11)$$

are “amputated”, that is, the tails in figure 1 correspond to field  $\phi$  and do not contain the factors  $\hat{G}$  that are present in the corresponding diagrams in  $Z[\mathbf{h}]$ . This is remedied by replacing  $\phi$  in (11) by  $\mathbf{h}\hat{G}$  in (9) and (10). Note that in the rightmost exponential an arbitrary quadratic term proportional to  $r$  has been introduced because of the arbitrariness in the definition of the interaction Hamiltonian as discussed in the previous section. It is compensated by  $r$  in  $G$  (7) so that  $Z[\mathbf{h}]$  in (3) does not depend on this parameter, as can be easily shown formally [13, 2, 4, 17].

One of the reasons for introducing the generating functional of S-matrix into the statistical theory was that the diagrams with  $l$  tails in the generating functional  $\ln Z[\mathbf{h}]$  include the product of  $l$  functions  $G(\mathbf{k})$ . In the critical region where all  $\mathbf{k}$  are small this factor strongly depends on the momenta which makes numerical approximations difficult. In contrast, the diagrams in  $U^R[\phi]$  are devoid of these factors and the amputated contributions admit approximation of the expansion coefficients by  $\mathbf{k}$ -independent constants, as, e.g., in CPA and DMFT. This property will be used below to introduce the LPA.

More important reason for using S-matrix is that it makes straightforward generalization of the effective medium approaches of the CPA and DMFT type to other cases, in particular, to the description of phase transitions [13, 2, 4, 17]. Formally the generalization is based on the exact expression for  $G^R$  obtained by substitution of (10) in (5):

$$G_{ij}^R = G_{ij} - G_{ii'}(u_2^R)_{i'j'}G_{j'j}. \quad (12)$$

This expression differs from (7) by the second term on the r.h.s. so for self-consistency of the theory it should vanish which means  $u_2^R = 0$ . From figure 1 it is seen that without the second diagram individual excitations can be perturbed only by other excitations but not by the medium within which they propagate. In this sense the medium can be called “effective”.

With constant  $r$  the effective medium condition can be satisfied only approximately. In the CPA and DMFT the approximation consists in assuming that the scattering is localized on the sites so that  $(u_2^R)_{ij} \propto \delta_{ij}$  and  $r$  (the coherent potential or the self-energy) is adjusted so that  $(u_2^R)_{i=j} = 0$ . The SSA, however, gives a very poor description in the vicinity of the critical point [2] that is why in the previous section the condition (8) has been suggested. As is easily seen by Fourier transforming (12) it amounts to

$$u_2^R(\mathbf{k} = 0) = 0. \quad (13)$$

Implementation of this condition requires explicit calculation of the long-wavelength limit of  $u_2^R$  which will be done below within a lattice generalization of the functional RG approach developed in [16] for  $n$ -vector models in the continuous space.

#### 4. The layer-cake renormalization scheme

As was pointed out earlier, the generating functional of S-matrix is convenient for approximate calculations so the RG equation will be derived with the use of (11) by casting it in the form

$$e^{-U^R[\phi]} = \exp\left(\frac{1}{2} \sum_{\mathbf{k}} \partial_{\phi_{\sigma,\mathbf{k}}} G(\mathbf{k}) \partial_{\phi_{\sigma,-\mathbf{k}}}\right) e^{-U^0[\phi]} \quad (14)$$

where

$$\phi_{\sigma,\mathbf{k}} = N^{-1/2} \sum_j e^{-ij \cdot \mathbf{k}} \phi_{\sigma j}. \quad (15)$$

and

$$U^0[\phi] = -\frac{r}{2} \phi_i \cdot \phi_i + H_I[\phi] + (\text{f.i.t.}). \quad (16)$$

Here and everywhere below (f.i.t.) stands for field-independent terms which will not be needed in calculations below. They, however, contribute to the absolute value of the free energy and should be included in the calculations if this quantity is of interest.

Fully renormalized  $U^R$  will be approximately calculated within the renormalization scheme developed in [16] for continuous space and adopted to the lattice case with the help of the layer-cake representation of the propagator  $G$  in (14). The layer-cake representation is defined only for non-negative functions [20], so we will assume that  $G(\mathbf{k}) > 0$  which is valid for all models discussed below. The representation is introduced by the identity

$$G(\mathbf{k}) = \int_0^{G(\mathbf{k})} dt' = \int_0^{t_{end}} \theta[G(\mathbf{k}) - t'] dt' \quad (17)$$

where  $t_{end} = 1/r$  is the maximum value of the evolution parameter  $t$  (see figure 2).

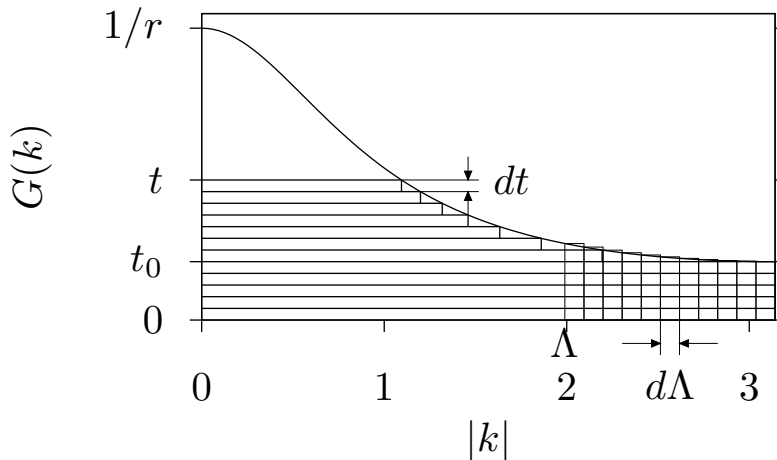


Figure 2: Schematic illustration of the difference between the infinitesimal elimination steps in the layer-cake (horizontal slices) and the Wilsonian (vertical slices) renormalization schemes shown for 1D propagator (7).

Integration over  $t'$  in (17) effectively splits the differential operator in (14) into infinitesimal contributions that can be used in the incremental renormalization procedure [5, 16]. In the layer-cake renormalization scheme the field components are integrated out layerwise [16], as shown in figure 2. Partly renormalized  $U[\phi, t]$  at intermediate “times” is defined by the equation

$$e^{-U[\phi, t]} = \exp\left(\frac{1}{2} \sum_{\mathbf{k}} \int_0^t \theta[G(\mathbf{k}) - t'] dt' \partial_{\phi_{\sigma, \mathbf{k}}} \partial_{\phi_{\sigma, -\mathbf{k}}}\right) e^{-U^0[\phi]} \quad (18)$$

so satisfies the functional-differential evolution equation

$$U'_t = \frac{1}{2} \sum_{\mathbf{k}} \theta[G(\mathbf{k}) - t] (\partial_{\phi_{\sigma, \mathbf{k}}} \partial_{\phi_{\sigma, -\mathbf{k}}} U - \partial_{\phi_{\sigma, \mathbf{k}}} U \partial_{\phi_{\sigma, -\mathbf{k}}} U). \quad (19)$$

with the initial condition  $U[\phi, t = 0] = U^0[\phi]$  in (16). Equation (19) has a form of the exact RG equations derived, e.g., in [5, 21] (see bibliography to more recent literature in [9, 6, 8, 10]) from which it differs only by the choice of the cut-off function and by the absence of the rescaling of variables often used to obtain the equations in scaling form. The rescaling of (19) could be easily done but it would introduce into the equation the largest critical exponent  $d$  which simply reflects the fact that the free energy grows with the linear system size  $L$  as  $L^d$ . Being the largest Lyapunov exponent of the equation, however, it would noticeably deteriorate its numerical solvability.

Equation (19) is exact and its solution could be used to obtain all CFs by differentiating (9) with respect to the source field. However, its exact solution is impossible for nontrivial models so approximations and simplifications are in order. One simplification is achieved by restricting consideration to only

homogeneous source field  $\mathbf{h}$  which in the momentum space will have only one non-zero Fourier component  $\mathbf{h}_{\mathbf{k}=\mathbf{0}}$ . Thus, to calculate magnetization in (31), only  $U^R[\phi_{\mathbf{k}=\mathbf{0}}]$  needs to be kept in (10). In view of this we will assume that all field components in (19) with the momenta outside the ‘‘Fermi surface’’ defined by the condition  $G(\mathbf{k}) = t$  or

$$\epsilon(\mathbf{k}) = t^{-1} - r \equiv E_F \quad (20)$$

will be set equal to zero so at  $t = t_{end}$  only the component  $\phi_{\mathbf{k}=\mathbf{0}}$  will survive. In this case the functional  $U^R$  effectively becomes a function of a single  $n$ -vector variable.

#### 4.1. The LPA

As was noted in the Introduction, the LPA is similar to the such approximations as CPA and DMFT in that currently it cannot be rigorously justified in the strong coupling case. (In the limit of weak coupling all approximations reproduce correctly the lowest-order perturbative terms so, on the one hand, the perturbation theory justifies them in this limit, on the other hand, makes them superfluous.) The gradient expansion [22, 23] frequently invoked to substantiate LPA is inapplicable in lattice models, so only heuristic arguments, such as those presented below, can be given to qualitatively understand, at least qualitatively, why LPA gives reasonable quantitative approximation to for such models, as will be illustrated by numerical calculations in section 5.

Thus, designating LPA as an approximation is somewhat misleading in the lattice case where it is rather an *ansatz* which consists in assuming that in models with the local initial  $U^0$  (16),  $U[\phi, t]$  will preserve the locality throughout the evolution described by the RG equation (19). The simplification achieved consists in that the functional of  $N \times n$ -dimensional lattice field can be fully characterized by a function  $u(\mathbf{x}, t)$  of one  $n$ -dimensional vector  $\mathbf{x}$  which in RG literature is usually called the local potential. To derive RG equation for  $u$  we first note that in Fourier representation (written here for simplicity for  $n = 1$ )

$$\begin{aligned} U[\phi, t] &= N \sum_{l=0}^{\infty} \sum_{\{\mathbf{k}_m\}} N^{-l/2} u_l(t) \delta \left( \sum_{m=1}^l \mathbf{k}_m \right) \frac{1}{l!} \prod_{m=1}^l \phi_{\mathbf{k}_m} \\ &\rightarrow u(x, t) = \sum_{l=0}^{\infty} u_l(t) \frac{x^l}{l!} \end{aligned} \quad (21)$$

(where  $\delta$ 's are the lattice Fourier transform of the Kronecker delta) the locality means that the expansion coefficients  $u_l(t)$  do not depend on the field momenta  $\mathbf{k}_m$ .

In this approximation the action of the second derivatives on the r.h.s. of (19) on each term in (22) amounts to the elimination of two field variables which momenta  $\mathbf{k}$  and  $-\mathbf{k}$  cancel out in the delta-function argument so all dependence

on  $\mathbf{k}$  separates into the factor common to all terms in the expansion

$$\begin{aligned} p(t) &= \frac{1}{N} \sum_{\mathbf{k}} \theta[G(\mathbf{k}) - t] = \frac{1}{N} \sum_{\mathbf{k}} \theta[t^{-1} - r - \epsilon(\mathbf{k})] \\ &= D_{tot}(t^{-1} - r) = \int_0^{t^{-1}-r} dE D(E). \end{aligned} \quad (22)$$

Here the second equality on the first line follows from the fact that the value of theta-function does not change when its argument is multiplied by the positive function  $[\epsilon(\mathbf{k}) + r]/t$  and the first equality on the second line follows from the observation that  $\theta$ -function is a  $T \rightarrow 0$  limit of the Fermi-function and thus the summation over momentum counts the total number of states below the ‘‘Fermi energy’’  $E_F$  (20) in the band with dispersion  $\epsilon(\mathbf{k})$  and so is equal to the integrated density of states  $D(E)$  at  $E_F$  [10, 17]. This makes possible to write down the first term in (19) in terms of function  $u$  as

$$\frac{1}{2} \sum_{\mathbf{k}} \theta[G(\mathbf{k}) - t] \partial_{\phi_{\sigma,\mathbf{k}}} \partial_{\phi_{\sigma,-\mathbf{k}}} U \rightarrow \frac{1}{2} p(t) \nabla^2 u(\mathbf{x}, t). \quad (23)$$

The second term on the r.h.s. of (19) is more convenient to analyze in the lattice coordinates. Substituting  $U$  in the LPA from (22) into the second term one gets

$$\begin{aligned} -\frac{1}{2} \sum_{\mathbf{k}} \theta[G(\mathbf{k}) - t] \partial_{\phi_{\sigma,\mathbf{k}}} U \partial_{\phi_{\sigma,-\mathbf{k}}} U &= -\frac{1}{2} U_{\phi_{\sigma,i}} \Delta_{ij} U_{\phi_{\sigma,j}} \\ &\rightsquigarrow -\frac{1}{2} [\nabla u(\mathbf{x}, t)]^2 \end{aligned} \quad (24)$$

where

$$\Delta_{ij} = \sum_{\mathbf{k}} \theta[G(\mathbf{k}) - t] e^{i\mathbf{k} \cdot (i-j)} \quad (25)$$

and the wiggly arrow means an approximate mapping, as explained below. If  $\theta$  in (25) is equal to unity in the whole BZ,  $\Delta_{ij}$  becomes equal to the conventional Kronecker delta and the term on the r.h.s. becomes strictly local and LPA is fully justified. This special case will be considered in the next subsection. However, as  $t$  evolves toward  $t_{end}$ ,  $\Delta_{ij}$  becomes progressively more and more spatially extended with characteristic half width  $O(1/k_c)$  where  $k_c$  is the maximum absolute value of the cutoff momenta at the Fermi surface (20). On the other hand,  $\Delta_{ij}$  remains peaked at  $i = j$ , it is symmetric in  $i$  and  $j$ , and is normalized to unity:  $\sum_{i(\text{or } j)} \Delta_{ij} = 1$ . Thus, it can be considered as a smeared approximation to the Kronecker delta which can be used to justify the approximation of the term on the r.h.s. of (24) by the squares of the local derivatives. Of course, from the mathematical standpoint the approximation severely worsens when  $k_c \rightarrow 0$  as  $t \rightarrow t_{end}$ . But we remind that in the process of elimination of high momentum components the nonzero field components  $\phi_{\mathbf{k}}$  also are restricted to the same momentum range  $|\mathbf{k}| \leq k_c$  so in the lattice coordinates

$\phi_{\sigma,i}$  as well as  $U(\phi_{\sigma,i})$  entering (24) are slowly varying functions of the lattice coordinates on the same scale  $O(1/k_c)$ . Thus, approximation  $\Delta_{ij} \approx \delta_{ij}$  in (24) may be quite consistent in this particular case. Besides, the gradient expansion [22, 23] which in the momentum space is equivalent to expansion in powers of  $\mathbf{k}_m$  may also be invoked to substantiate LPA in the region of small momenta.

Substituting (23) and (24) in (19) one arrives at the equation

$$u_t = \frac{1}{2} [p(t)\nabla_{\mathbf{x}}^2 u - (\nabla_{\mathbf{x}} u)^2]. \quad (26)$$

which is the lattice generalization of the LPA equation derived in [16].

#### 4.2. Exact partial renormalization

Differential equations of the form (26) currently cannot be solved analytically for arbitrary  $p(t)$ , so numerical solutions should be used. However, even numerical treatment meets with difficulties in some cases. For example, in the case of the *spin* models when the initial Hamiltonian (A.1) is singular and is not differentiable numerically. Fortunately, when  $p(t) = \text{Const}$  equation (26) is exactly solvable which can be used to regularize the initial conditions as follows.

From the definition of  $p$  (22) it can be seen that for sufficiently small  $t$  the ‘‘Fermi energy’’  $t^{-1} - r$  will exceed the width of the quasiparticle band that extends from zero to  $\max_{\mathbf{k}} \epsilon(\mathbf{k})$  the integrated densities of states (DOS) will be equal to its maximum unit value when  $t$  satisfies

$$0 \leq t \leq t_0 = \min_{\mathbf{k}} G(\mathbf{k}) = \frac{1}{\max_{\mathbf{k}} \epsilon(\mathbf{k}) + r} \quad (27)$$

(see figure 2). In this range equation (26) with  $p = 1$  by substitution  $e^{-u}$  can be transformed to the  $n$ -dimensional linear diffusion equation which solution with the use of the diffusion kernel reads

$$e^{-u(\mathbf{x},t_0)} = \frac{1}{(2\pi t_0)^{n/2}} \int d\mathbf{x}_0 \exp\left(-\frac{(\mathbf{x} - \mathbf{x}_0)^2}{2t_0}\right) e^{-u^0 \mathbf{x}} \quad (28)$$

where  $u^0$  is the potential corresponding to (16).

Thus, in the case of local Hamiltonians the RG equations,—both, exact and approximate,—can be integrated from  $t_0$  to  $t_{end} = 1/r$  with the initial condition (28) (for the exact equation the inverse map  $u(\mathbf{x}, t_0) \rightarrow U[\phi, t_0]$  should be performed). It is pertinent to note here that when  $r$  becomes large, the integration span  $\Delta t = t_{end} - t_0$  shrinks as  $\sim 1/r^2$ . Function  $G(\mathbf{k})$  flattens and a good approximation can be obtained by neglecting its  $\mathbf{k}$ -dependence and approximating  $G(\mathbf{k})$  by its average

$$g = N^{-1} \sum_{\mathbf{k}} G(\mathbf{k}). \quad (29)$$

In this case integration over  $t$  in (19) and (26) is not needed anymore because renormalized  $U^R$  and  $u^R$  are given by (28) with  $t_0 = g$ . Augmenting this

with the self-consistency condition  $(u_2^R)_{i=j} = 0$  (see (12)) one arrives at the SSA such as the CPA [13, 2]. In the case of large  $r$  it is straightforward to calculate corrections to the SSA. Formally (14) can be seen as a closed form of the perturbative expansion so by choosing in (28)  $t_0 = g$  and simultaneously subtracting  $g$  from  $G$  in (14) one arrives at the expansion with the renormalized local potential (28) and the propagator [13, 2].

$$\tilde{G}(\mathbf{k}) = G(\mathbf{k}) - g. \quad (30)$$

When  $r$  is large the deviations of  $G\mathbf{k}$  from  $g$  will be small (see figure 2) so  $\tilde{G}$  can be used as an expansion parameter. The Feynman diagrams in this expansion would simplify because the tadpole contributions will be implicitly accounted for by the redefined propagator (30) which is similar to the normal ordering in quantum many-body theory. So the relative importance of the correction terms will be defined by the number of propagator lines  $\tilde{G}(\mathbf{k})$  in the corresponding diagrams.

## 5. Numerical results

The LPA RG equation (26) could be readily integrated in the symmetric phase but below the critical temperature  $T_c$  the solution exhibited singular behavior due to the physics of the phase coexistence region. In the  $n = 1$  case this can be easily understood as follows (see discussion of this point in the RG context in [24, 25]). In the zero external field the statistical ensemble below  $T_c$  consists of a mixture of two pure phases with saturated magnetizations  $\pm m_0$  so in the coexistence region the magnetization may take any value in the interval  $m \in [-m_0, m_0]$ . But an infinitesimal external field  $h = 0^\pm$  will bring the magnetization either to  $m_0$  or to  $-m_0$  which in the case  $m \neq \pm m_0$  means infinite susceptibility. However, if the magnetization is saturated and is equal, e.g., to  $m_0 > 0$  and the infinitesimal field also is positive the susceptibility will remain finite which means discontinuity at  $h = 0$  because for  $h = 0^-$  magnetization will jump to the value  $-m_0$ .

According to (4), in the LPA the magnetization in the homogeneous (ferromagnetic) Ising model ( $n = 1$ ) is

$$m = \frac{1}{N} \frac{\partial \ln Z(h)}{\partial h} = x - u_x^R/r \quad (31)$$

where  $x = h/r$ ,  $u^R = u(x, t_{end})$  and in the last equality use has been made of equations (9), (11), (22) and (7). The susceptibility is found from (31) as

$$\chi = m_h = \frac{1}{r} - \frac{1}{r^2} u_{xx}^R. \quad (32)$$

At a finite distance from  $T_c$  the correlation length, hence,  $1/r$  remain finite, so it is the second derivative in (32) that is responsible for the infinite value of  $\chi$ .

The origin of the singularity can be understood from the particular solution of equation (26)

$$u^G(\mathbf{x}, t) = \frac{\mathbf{x}^2}{2(t - t_{end})} + (\text{f.i.t.}). \quad (33)$$

It formally corresponds to the Gaussian model but is non-physical because  $t$  is always smaller than  $t_{end}$  so the Hamiltonian corresponding to (33) is not bounded from below. However, it may be useful to qualitatively understand the singularity in the solution for physical models because below  $T_c$  all  $u^0(\mathbf{x})$  (see, e.g., Appendix A) have negative curvature near  $\mathbf{x} = 0$  and their solutions may develop behavior similar to (33) (above  $T_c$  the negative curvature does not survive the renormalization and becomes positive at  $t = t_{end}$ ).

The unbounded derivatives in  $\mathbf{x}$  and  $t$  indeed arose in the numerical solutions of the LPA equation (26) which made it difficult to deal with numerically below  $T_c$ . Fortunately, the singularities disappear under the Legendre transform given by equations (B.1) and (B.2) which are a  $t$ -dependent generalization of the transform suggested in [26]. Under the transform the Gaussian solution (33) takes the form

$$v^G(\mathbf{y}, t) = -\frac{\mathbf{y}^2}{2\Delta t} + (\text{f.i.t.}), \quad (34)$$

in which all terms are bounded.

Though in the symmetric phase equation (26) can be integrated for any  $n$ , it showed lesser stability near the critical point than the transformed equations, presumably because of the closeness to the ordered state. Therefore, in the calculations below the transformed equations will be used both above and below  $T_c$ .

### 5.1. The symmetric phase

In the symmetric phase the transformed equation derived from (B.9), (B.10) and (B.13) reads

$$w_t = \frac{p(t)}{2} \left( \frac{(n-1)w_q}{1 + (t-t_0)w_q} + \frac{w_q + 2qw_{qq}}{1 + (t-t_0)(w_q + 2qw_{qq})} \right) \quad (35)$$

where the arbitrary constant  $c$  was chosen to be equal to  $t_0$ . With this choice the initial condition is easily found from (B.1), (B.2) and (B.10) as

$$w(q, t_0) = u(\sqrt{2q}, t_0) \quad (36)$$

with  $u(\mathbf{x}, t_0)$  calculated in Appendix A; here the superscript “ $(n)$ ” was omitted for consistency with (35) which holds for all  $n \geq 1$ .

The self-consistency condition (13) in the fully symmetric case means that all derivatives  $u_{x_\sigma x_{\sigma'}}$  in (B.7) vanish so all  $v_{y_\sigma y_{\sigma'}}$  are also equal to zero. In the  $O(n)$ -symmetric case this leads via (B.11) to

$$w_q^R|_{q=0} = 0. \quad (37)$$

Equation (35) and (37) with the initial condition (36) has been solved numerically for the  $n$ -vector spin models with

$$\epsilon(\mathbf{k}) = K \sum_{i_{NN}} (1 - e^{i\mathbf{k} \cdot i_{NN}}) \quad (38)$$

where  $K = |J|/k_B T$  ( $J$  the ferromagnetic coupling between NN spins) and  $\{i_{NN}\}$  are the lattice vectors connecting the site at the origin with all NN sites.

In the calculations  $D_{tot}(E)$  for dispersions (38) were obtained with the use of the expressions derived in [27] for the DOS of SC, BCC and FCC lattices. For general dispersion straightforward numerical integration of (22) by the Monkhorst-Pack method [28] can be efficient because the integrated DOS  $D_{tot}(E)$  is much less structured than the DOS itself. In case of necessity, the region of small  $|\mathbf{k}|$  near the bottom of the band where  $\epsilon(\mathbf{k}) \propto \mathbf{k}^2$  can be treated analytically. Thus, application of the LPA to the pair spin interactions of arbitrary range [1, 29, 30] should cause no problems.

The LPA equations have been solved by the method of lines with the use of the Fortran LSODE routine [31]. The number of equations used varied in the range 2-4 thousands until convergence has been reached. Qualitative behavior of the solutions both in the symmetric and in the ordered phases agreed with the results of previous studies [24, 25, 17]. Near the critical temperature  $t_{end} = 1/r \rightarrow \infty$  but in numerical integration the interval is necessarily bounded so  $K_c$  was found by extrapolating several  $r$  calculated at  $K \gtrsim K_c$  to  $r = 0$  according to the scaling relation

$$r = C_{\pm}^{-1} \tau^{2\nu} = C_{\pm}^{-1} \tau^{\gamma} \quad (39)$$

where  $\tau = |1 - K_c/K|$  and  $\gamma = 2\nu$  because in the LPA  $\eta = 0$ . The correlation length in the Ising model both above (+) and below (-)  $T_c$  has been estimated on the basis of the asymptotic behavior of  $G$  in real space which can be found by the inverse Fourier transform of (7)

$$\xi = \sqrt{K/r} \stackrel{T \rightarrow T_c}{\simeq} f_{\pm} \tau^{-\nu}. \quad (40)$$

For consistency, the critical exponents  $\nu$  were found from the scaled form of the RG equation (35) as explained in [16]. The obtained values of  $\nu$  were equal to 0.65 for  $n = 1$ , 0.71 for  $n = 2$  and 0.76 for  $n = 3$  and were similar but larger than those systematized in table 2 in [6]. They were closest to the values of  $\nu$  calculated in [6] by being larger on 0.01. This apparently is a consequence of a similar non-perturbative RG approach used by the authors. The difference caused by the difference in  $\eta$  which in the calculations of [6] was not equal to zero but obtained from RG equations.

The calculated values of  $K_c$  at the critical point found with the use of equations (35) are presented in table 1.

### 5.2. Ordering in the Ising model

According to (4), to calculate the spontaneous magnetization in zero external field we still need to take into account the source field  $h$ . In the  $n = 1$  case the

Table 1: Dimensionless inverse critical temperatures of the  $n$ -vector spin models on cubic lattices calculated in the LPA. The errors have been estimated by comparison with data from MC simulations [32] for  $n = 1$  (the Ising model) and with the high temperature expansion for  $n = 2$  and 3 [33].

$n$	Lattice	$K_c$	Error
1	FCC	0.1023	0.2%
1	BCC	0.1579	0.3%
1	SC	0.2235	0.8%
2	BCC	0.3225	0.6%
2	SC	0.4597	1.2%
3	BCC	0.4905	0.8%
3	SC	0.7025	1.4%

Legendre transform (Appendix B) simplifies to

$$y = x - (t - t_0)u_x \quad (41)$$

$$v = u - \frac{1}{2}(t - t_0)u_x^2 \quad (42)$$

where the arguments of  $u(x, t)$  and  $v(y, t)$  have been omitted for brevity and constant  $c$  was chosen to be equal to  $t_0$  because with this choice there is no need to perform numerical Legendre transform of the initial condition (A.2) needed in some renormalization schemes [10]:

$$v(y, t_0) = u^{(1)}(x, t_0)|_{x=y}. \quad (43)$$

The RG equation in this case reads (see Appendix B)

$$v_t = \frac{p(t)v_{yy}}{2[1 + (t - t_0)v_{yy}]}. \quad (44)$$

The dependence of  $v^R$  on  $h$  at the end of renormalization is defined parametrically with the use of the expression for  $h$

$$x = h/r = y + \Delta t v_y^R \quad (45)$$

which follows from (41) and (B.6) with  $t = t_{end}$ . The unknown parameter  $r = 1/t_{end}$  in (45) is fixed by the self-consistency condition (13) which according to (B.7) and (B.15) now reads

$$v_{yy}^R|_{h=0+} = 0 \quad (46)$$

where  $h$  should be expressed through  $y$  according to (45). At  $h = 0$  there always exists a trivial solution  $y = 0$  due to the symmetry. But below  $T_c$  two stable solutions with  $y = \pm y_0 \neq 0$  appear which correspond to the states with spontaneous magnetization

$$m_0 = y_0 - t_0 v_y^R|_{y_0} \quad (47)$$

as can be found from (31), (45) and (B.6).

Numerically found solution of equation (44) with the initial condition (43) and the self-consistency condition (46) exhibited the same qualitative behavior as found previously in [25]. Namely, the inverse susceptibility was equal to zero in the interval  $(0, m_0)$  (the solution for negative  $m$  can be obtained by symmetry) and jumped to  $\chi^{-1} = r$ , at  $m_0$ , in accordance with (B.16). In particular, it was found that the Gaussian solution (34) describes the solution for the Ising model in the ordered phase so accurately that the precision of the calculations was insufficient to see the difference. This can be partly explained by the fact that the  $y$ -dependent part of (34) is stationary and from (44) it can be seen that small  $y$ -dependent deviations from  $v^G$  do not grow when  $t \rightarrow t_{end}$  so (34) might have been a fixed point of the LPA RG equation if  $t \rightarrow \infty$ . However, in the SC-LPA the largest  $t$  is equal to  $t_{end} = 1/r$  which away from the critical point is finite. So the close proximity of the solution to the Gaussian model seen in the calculations might be due to relatively large values of  $t_{end}$  in our calculations performed in the region within 10% distance from  $T_c$ .

Similarly, it was impossible to establish numerically whether the discontinuity in the inverse susceptibility is genuine or is just a very steep continuous transition (see discussion in [25]). But anyway the LPA is not exact, so taking into account the narrowness of the finite difference step in  $\Delta y = O(10^{-3})$  within which the inverse susceptibility changed from zero to  $r$  and the fact that the exact behavior is well understood qualitatively, the approximately correct behavior obtained numerically can be fitted to the exact one with the use of an analogue of the Maxwell construction appropriately adopted to this case (cf. [24]).

In the calculations the value of  $m_0$  has been calculated from (47) at the point  $y_0$  where both conditions (45) with  $h^+ = 0$  and (46) has been satisfied by appropriate choice of  $r$ . The possibility to satisfy two conditions with one adjustable parameter was due to the fact that the jump occurs only in  $v_{yy}^R$  but  $v_y^R$  is continuous. And because the Ising model solution for  $y \leq y_0$  coincided with the Gaussian solution (34),  $h$  in (45) was equal to zero everywhere in the interval  $[0, y_0]$  including the endpoint, so effectively only the self-consistency condition (46) had to be satisfied.

The magnetization curve obtained by the above procedure is shown in figure 3 together with the exact MC simulations data from [34] accurately described by the expression

$$m_0(\tau) = \tau^\beta (a_0 - a_1 \tau^{\theta_W} - a_2 \tau) \quad (48)$$

This expression has been also fitted to LPA curve but with  $\beta$  equal to  $\beta_{LPA} = \nu/2$  and the Wegner exponent  $\theta_W$  set to 0.5 [34]. In table 2 the parameters of both fits are compared. As is seen, the LPA parameters  $a_{1-2}$  deviate quite appreciably from the (rounded) exact values of [34] but it has to be born in mind that the parameters refer to the correction terms that enter (48) multiplied by positive powers of  $\tau$ . The latter was smaller than 0.1 in the calculations so, on the one hand, the contribution of the terms to the magnetization curve was reduced by these factors, on the other hand, their fit for the same reason was not

Table 2: The amplitudes entering the scaling relations (39), (40) and (48) calculated in the present work compared with the high temperature expansions data of [35] ( $C_{\pm}, f_{\pm}$ ) for  $\gamma = 1.25$  which is closest to the LPA value 1.3 and with the MC simulations of [34] ( $a_0 - a_2$ ).

	$C_+$	$f_+$	$C_-$	$f_-$	$a_0$	$a_1$	$a_2$
LPA	1.06	0.487	0.21	0.22	1.62	0.23	0.37
[35, 34]	1.06	0.485	0.21	0.25	1.69	0.34	0.43

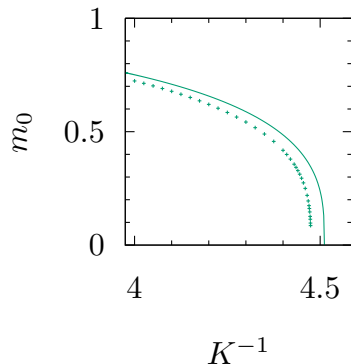


Figure 3: Magnetization curve near the critical point as obtained in the LPA (symbols) and the fitting curve (48) to the exact MC simulations with the parameters from [34] (solid line).

very accurate and might improve with improved precision of the calculations.

The temperature range in the simulations was restricted to 10% distance from  $T_c$  for the following reasons. First, the correlation length at the lowest temperature  $\sim 0.8$  l.u. was already smaller than the lattice constant which means that the system was far from the critical region which was of the main interest in the present study. Second, at lowering temperature the numerical integration considerably slowed down so that convergence to the self-consistent solution by iterations was difficult to achieve. It is quite possible, however, that the SC-LPA can describe the low-temperature magnetization in an asymptotically exact way. As  $T \rightarrow 0$ ,  $r$  grows very fast so  $G(\mathbf{k})$  flattens (see section 4.2) and the SSA should be adequate. It does reproduce correctly the leading asymptotic correction to the saturated magnetization  $m_0 = 1$  and the LPA may follow the suite. However, at low temperatures  $r$  grows by the Arrhenius law  $r \propto e^{AK}$  with  $A = O(10)$  so the integration range shrinks as  $1/r \sim e^{-AK}$  and at the same time the second derivative  $u_{xx}^0$  in (A.2) grows as  $r^2$  which poses serious computational problems. Presumably, an analytic expansion of the kind discussed in section 4.2 or in [13] would be more suitable in the low-temperature region.

### 5.3. Ordering in beta brass

As is known, the Ising model on a bipartite lattice in zero external field ordered antiferromagnetically can be mapped onto ferromagnetic model by flipping the spins on every second site and simultaneously changing signs of the

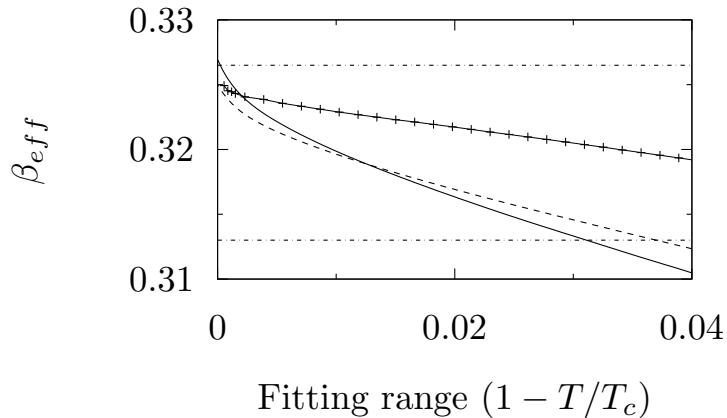


Figure 4: Symbols (the line is to guide the eye): exponent  $\beta$  as obtained by the fit of the scaling law  $m_0 \propto \tau^{\beta_{eff}}$  within the interval  $0 - \tau$  to the magnetization  $m_0$  calculated with the use of the SC-LPA equations for the BCC Ising model; solid and dashed lines: same fit to equation (48) with the parameters taken from the second and the first lines in table 2, respectively; the upper horizontal dashed-dotted line is the best known universal value for the exponent [8], the lower line is the value used in [11].

spin interactions in such a way that the value of the Hamiltonian remained unchanged. So the formalism developed for the ferromagnetic case is fully applicable to the ordering of, e.g., an equiatomic BCC alloy, such as the beta brass [11].

The interpretation of the experimental data on ordering in this alloy on the basis of approximate solutions of the NN Ising model showed an overall good agreement with experiment (see [11] and references therein). However, theoretical value  $\beta = 0.313$  of the order parameter exponent used by the authors was about 4% smaller than the value  $\beta = 0.3265$  predicted by the RG theory [8] though it fitted well experimental data in the  $\gtrsim 1\%$  vicinity of  $T_C$ . In a broader fitting range  $0 < \tau < 0.04$  the difference was even larger ( $\gtrsim 10\%$ ) [11]. The reason for the discrepancy apparently lies in the inevitably finite temperature intervals near  $T_c$  used in experimental measurements while the RG predictions are strictly valid only infinitesimally close to the critical temperature. Thus, explanation for the deviation of the experimental values from RG theory should be sought in the influence of non-universal contributions.

Indeed, by fitting expression (48) to the scaling form with an effective exponent  $\beta_{eff}$  (see figure 4) one finds noticeable deviation from the RG value, though not as large as observed experimentally.

Though the LPA calculations shown in figure 4 do not agree with the experimental data on  $\beta$  [11] quantitatively, the deviations from the RG value are of similar order of magnitude. Also, their absolute value grows with the widening of the fitting range qualitatively similar to findings in [11] and are of the correct sign. The latter point is quite nontrivial because it is usually expected that

when going away from the critical point the system tends to exhibit the mean-field behavior [5] with  $\beta_{MF} = 0.5 > \beta$ . So *a priori* one would expect  $\beta_{eff} > \beta$  in contradiction to experiment but in accordance with the LPA and with the exact MC simulations [34]. Also noticeable is the fact that though the SC and BCC Ising models differ in the critical region only by irrelevant variables, as is seen from figure 4, the deviation of  $\beta_{eff}$  from  $\beta$  is quite different in the two cases which means that the influence of irrelevant variables is strong. On the other hand, from the results of the band structure theory of order in alloys it looks highly implausible that the ordering potential would be accurately represented by the NN Ising model [1, 29]. Much more likely that the pair interactions would extend on many coordination spheres and also multi-site cluster interactions may contribute to the ordering. Therefore, the non-universal contributions can be very different from the simple NN case used in the calculations shown in figure 4 and might be strong enough to bring the LPA values of  $\beta_{eff}$  close to those found in [11].

## 6. Discussion

Numerical calculations of the last section have shown that the self-consistent RG equation derived in the present Letter make possible calculation of non-universal quantities in  $n$ -vector spin models within LPA in good agreement with the values known from reliable techniques such as the high-temperature expansions and the Monte Carlo simulations [33, 34, 32]. The accuracy of calculation of the critical temperatures can be sufficient to many practical purposes, e.g., in application to phase equilibria in alloys where the errors in microscopic Hamiltonian parameters determined either theoretically or experimentally [1, 29, 30] are currently larger than 0.2 – 0.3% errors in the LPA values of  $T_c$  for BCC and FCC Ising models (see table 1).

The main deficiency of the SC-LPA approach is that, similarly to CPA and DMFT, it is a closed-form approximation which cannot be rigorously justified and/or improved in the strong coupling case (in the case of weak coupling all effective medium theories are exact to the leading order in the interaction and are normally superfluous). As was mentioned in the Introduction, a natural way of going beyond the SSA such as CPA and DMFT by analogy with which SC-LPA has been devised is to resort to their cluster generalizations which can be systematically improved and which are based on the same self-consistency condition [13, 2, 3] as the SSA thus making generalization relatively straightforward. Schematically this can be done as follows. First, in (30) constant  $g$  should be replaced by a function of  $\mathbf{k}$  consisting of a finite sum of the lattice Fourier terms

$$g(\mathbf{k}) = \sum_{|l| \leq L_c} g_l e^{il \cdot \mathbf{k}} \quad (49)$$

where  $L_c$  is some spatial cut-off so in the lattice coordinated the matrix elements  $g_{ij}$  will vanish beyond the cluster of radius  $L_c$ :  $g_{ij}|_{|i-j| > L_c} = 0$ . Now, if the system is far from criticality the matrix elements of the propagator  $G$

will exponentially attenuate at large separations [13] and may be neglected for  $|i-j| > L_c$  with the accuracy  $O(e^{-L_c/\xi})$ . In such a case by choosing  $g_l \simeq G_{i-j=l}$  in (49) one may neglect  $\tilde{G}$  in (30) so the partition function can be calculated by the cluster techniques with the use of the clusters of radius  $\simeq L_c$  (see [2, 4]).

As is easy to see, the approximation will break down in the critical region. For example, at the critical point  $G$  in (7) is singular at  $\mathbf{k} = 0$  but no finite Fourier sum (49) will reproduce the singularity. Still, one can choose  $g_l$  in (49) in such a way that  $g(\mathbf{k})$  will satisfactorily approximate  $G(\mathbf{k})$  everywhere in BZ with the exception of a region surrounding  $\mathbf{k} = 0$  with  $|\mathbf{k}| < k_c$ , where the cut-off  $k_c \sim 1/L_c$ . Now the contributions due to  $g$  can be calculated within the cluster method while the remaining singular part  $\tilde{G}$  for  $|\mathbf{k}| < k_c$  accounted for by the layer-cake renormalization and the LPA with the initial local potential taken from the cluster calculation (e.g., by setting the momenta at the vertices to zero). Within this approach the low- $\mathbf{k}$  region will shrink with the growing cluster radius  $L_c$  which would diminish the LPA contribution thus making the calculation more accurate because the larger cluster part should converge to the exact solution. Besides, smaller  $k_c$  means smaller renormalized interactions which will make LPA more reliable which is exact to the first order in the interactions [16]. Thus, with the use of this hybrid cluster/LPA approach the results obtained can be validated without resort to the high-temperature expansions or MC simulations. The feasibility of the approach is supported by the fact that in the purely cluster approach good convergence could be seen in several cases with the use of small easily manageable clusters [2, 4]. Finally, it is pertinent to note that besides making the LPA-based approach self-contained, the hybrid technique would enable dealing with the short-range cluster interactions that appear in the *ab initio* theory of alloys [1, 29]. This opens a possibility of developing a theory which would make possible a realistic description of the first- and the second-order phase transitions in lattice systems.

Another deficiency of the LPA is that it does not reproduce correctly the critical exponents. This problem is not very severe because the exponents are meaningful only asymptotically close to the critical point where the renormalized Hamiltonian simplifies, acquires a universal form and, most importantly, becomes of a weak-coupling kind in 3D case [5]. So the layer-cake renormalization can be stopped at sufficiently large value of  $t_c$  and the remaining renormalization performed with rigorous perturbative techniques [36, 37]. The necessary Feynman diagrams with  $\tilde{G}$  (30) can be reduced to the known expressions by separating  $\tilde{G}$  into  $G$  and  $g$ . The advantage of this approach would be that all necessary input parameters [36, 37] will be known to a good accuracy from the SC-LPA solution at  $t_c$ .

It should be noted that even in its simplest form the SC-LPA can be useful in interpreting experimental data on the critical behavior. As was shown in section 5.3, the non-universal contributions can considerably distort the observed value of the exponent  $\beta$  and SC-LPA can describe the deviation of  $\beta_{eff}$  from  $\beta$  reasonably well, as comparison with the exact MC simulations for the SC case shows (see figure 4). Qualitatively similar deviations were observed in

experiments on the ordering in beta-brass [11] but they were larger than in our calculations. While theoretically the value of  $\beta$  for the Ising universality class is known with the accuracy from three to four significant digits [8], in some fits in [11] even the first digit in  $\beta_{eff}$  did not agree with the RG value. Quantitative explanation of this discrepancy requires knowledge of the ordering potential for beta-brass which can be obtained either in *ab initio* calculations or from the diffuse scattering data [1, 29, 30]. Such explanation, besides resolving the issue with the value of  $\beta$  in beta-brass, would also test the ability of the SC-LPA to quantitatively describe non-universal behavior at finite distances from critical points in realistic situations, thus extending the use of the RG method beyond the immediate vicinity of the critical point.

### Acknowledgment

I would like to express my gratitude to Hugues Dreyssé for support and encouragement.

### Appendix A. Initial condition in the spin models

The spin models differ from the general  $n$ -vector case in that the length of vectors  $\mathbf{s}_i$  is fixed, for example, is equal to unity [33]. In the functional integral representation (3) this can be taken into account by the product of the Dirac delta-functions as

$$e^{-H_I} = \prod_i \delta(\mathbf{s}_i^2 - 1) = \lim_{u_4 \rightarrow \infty} \left( \frac{u_4}{\pi} \right)^{N/2} e^{-u_4 \sum_i (\mathbf{s}_i^2 - 1)^2} \quad (\text{A.1})$$

where the second equality shows that the spin Hamiltonian (1) formally corresponds to  $\phi^4$  model with infinitely strong interaction. Equation (26) would be difficult to integrate numerically in this case so partial exact renormalization described in section 4.2 is in order.

The  $n = 1$  case is trivial

$$u^{(1)}(\mathbf{x}, t_0) = \frac{x^2}{2t_0} - \ln \cosh \frac{x}{t_0} + (\text{f.i.t.}) \quad (\text{A.2})$$

where  $x = |\mathbf{x}|$  and (f.i.t.) stands for  $x$ -independent terms.

For  $n > 1$  in the  $O(n)$  symmetric case the integral in (28) is convenient to calculate in hyperspherical coordinates. Choosing the direction of  $\mathbf{x}$  along the first axis  $\mathbf{x} = (x \cos \theta, 0, 0, \dots, 0)$  one gets [38]

$$e^{-u^{(n)}(\mathbf{x}, t_0)} \propto e^{-\frac{x^2}{2t_0}} \int_0^\pi e^{\frac{x}{t_0} \cos \theta} \sin^{n-2} \theta d\theta. \quad (\text{A.3})$$

The cases  $n = 2$  and  $n = 3$  are given by

$$\begin{aligned} u^{(2)}(\mathbf{x}, t_0) &= \frac{x^2}{2t_0} - \ln I_0 \left( \frac{x}{t_0} \right) + (\text{f.i.t.}) \\ u^{(3)}(\mathbf{x}, t_0) &= \frac{x^2}{2t_0} - \ln \left( \frac{t_0}{x} \sinh \frac{x}{t_0} \right) + (\text{f.i.t.}) \end{aligned} \quad (\text{A.4})$$

where  $I_0$  is the modified Bessel function of the first kind.

Explicit expressions for  $n > 3$  is not considered in the main text so we only note that at large  $n > 8$  a three-term recurrence relation for integrals in (A.3) can be established so additionally only  $n = 4 - 8$  integrals will need to be calculated explicitly for  $n > 3$ .

## Appendix B. Transformed RG equation

In our case the Legendre transform suggested in [26] (see also [15]) should be modified as

$$y_\sigma(\mathbf{x}, t) = x_\sigma - (t - c)u_{x_\sigma}(\mathbf{x}, t) \quad (\text{B.1})$$

$$v(\mathbf{y}, t) = u(\mathbf{x}, t) - \frac{1}{2}(t - c) \sum_\sigma u_{x_\sigma}^2(\mathbf{x}, t) \quad (\text{B.2})$$

where  $\sigma = 1, \dots, n$  and  $c$  is an arbitrary constant. Here the independent variables are  $\mathbf{x}$  and  $t$  and the local potential is  $u$ . Our aim is to use these relations to re-write (26) in terms of  $\mathbf{y}$  and  $t$  for the transformed potential  $v$ . To this end we first differentiate Eqs. (B.1) and (B.2) with respect to  $x_{\sigma'}$ :

$$\frac{\partial y_\sigma}{\partial x_{\sigma'}} = \delta_{\sigma\sigma'} - (t - c)u_{x_\sigma x_{\sigma'}} \quad (\text{B.3})$$

$$v_{y_\sigma} \frac{\partial y_\sigma}{\partial x_{\sigma'}} = u_{x_{\sigma'}} - (t - c)u_{x_\sigma} u_{x_\sigma x_{\sigma'}}. \quad (\text{B.4})$$

(summation over repeated subscripts is assumed). Substituting (B.3) into (B.4) after some rearrangement one arrives at a linear system

$$[\delta_{\sigma\sigma'} - (t - c)u_{x_\sigma x_{\sigma'}}](v_{y_{\sigma'}} - u_{x_{\sigma'}}) = 0. \quad (\text{B.5})$$

Because the matrix in this equation is not singular in general case, it follows that for all  $\sigma = 1, \dots, n$

$$v_{y_\sigma} = u_{x_\sigma}. \quad (\text{B.6})$$

Differentiation of this with respect to  $x_{\sigma'}$  and using (B.3) gives

$$[\delta_{\sigma\kappa} + (t - c)v_{y_\sigma y_\kappa}]u_{x_\kappa x_{\sigma'}} = v_{y_\sigma y_{\sigma'}}. \quad (\text{B.7})$$

As is seen, by the matrix inversion all  $u_{x_\sigma x_{\sigma'}}$  in the LPA equation can be expressed in terms of  $v_{y_\kappa y_{\kappa'}}$ .

Finally, differentiating Eqs. (B.1) and (B.2) by  $t$  and using Eq. (B.6) one gets

$$u_t + \frac{1}{2} \sum_\sigma u_{x_\sigma}^2 = v_t \quad (\text{B.8})$$

(note the difference with equation (15) in [26] where the second term on the l.h.s. is absent) so that (26) can be written as

$$v_t = \frac{1}{2}p(t)u_{x_\sigma x_\sigma} = \frac{1}{2}p(t)\nabla_{\mathbf{x}}^2 u \quad (\text{B.9})$$

where the r.h.s. should be expressed in terms of  $v_{y_\sigma y_{\sigma'}}$  with the use of (B.7).

*Appendix B.1.  $O(n)$  symmetric case*

In a fully  $O(n)$  symmetric case (B.7) can be solved explicitly as follows. Introducing notation

$$v(\mathbf{y}, t) = w(q, t) \text{ where } q = \mathbf{y}^2/2 \quad (\text{B.10})$$

one finds

$$v_{y_{\sigma'} y_{\sigma}} = \delta_{\sigma' \sigma} w_q + y_{\sigma'} y_{\sigma} w_{qq}. \quad (\text{B.11})$$

Now denoting the matrix in (B.7) as  $\hat{M}$  with the use of (B.11) one gets

$$\begin{aligned} M_{\sigma\kappa} &= \delta_{\sigma\kappa} + (t - c)v_{y_{\sigma} y_{\kappa}} \\ &= [1 + (t - c)w_q] \left[ \delta_{\sigma\kappa} + y_{\sigma} y_{\kappa} \frac{(t - c)w_{qq}}{1 + (t - c)w_q} \right] \end{aligned} \quad (\text{B.12})$$

Substituting this in (B.7) and solving for  $u_{x_{\sigma} x_{\sigma'}}$ , one arrives at the expressions that eliminates  $u$  and  $\mathbf{x}$  on the r.h.s. of (B.9) as

$$\nabla_{\mathbf{x}}^2 u = \frac{(n - 1)w_q}{1 + (t - c)w_q} + \frac{w_q + 2qw_{qq}}{1 + (t - c)(w_q + 2qw_{qq})}. \quad (\text{B.13})$$

*Appendix B.2.  $n = 1$  case*

In the case  $n = 1$  the introduction of  $q$  is superfluous because directly from (B.7) one gets [26]

$$u_{xx} = \frac{v_{yy}}{1 + (t - c)v_{yy}}. \quad (\text{B.14})$$

Substituting this into (B.9) one obtains equation (44) of the main text. From (B.1) and (B.2) it is seen that the most convenient choice of the arbitrary constant is  $c = t_0$  so that there is no need in the Legendre transform of the initial variables. Now rewriting (B.14) as

$$\frac{1}{u_{xx}} = \frac{1}{v_{yy}} + t - t_0 \quad (\text{B.15})$$

it can be seen that if at some point  $t \neq t_0$   $u_{xx} \rightarrow \infty$   $v_{yy}$  remains finite:  $v_{yy} = -1/(t - t_0)$ .

Substituting (B.15) into (32) one finds the expression for the inverse susceptibility in the transformed variables

$$\chi^{-1} = \frac{1 + \Delta t v_{yy}^R}{1 - t_0 v_{yy}^R} r. \quad (\text{B.16})$$

**References**

**References**

- [1] F. Ducastelle, Order and Phase Stability in Alloys, North-Holland, Amsterdam, 1991.

- [2] V. I. Tokar, A new cluster method in lattice statistics, *Comput. Mater. Sci.* 8 (1997) 8–15.
- [3] T. Maier, M. Jarrell, T. Pruschke, M. H. Hettler, Quantum cluster theories, *Rev. Mod. Phys.* 77 (2005) 1027–1080.
- [4] T. L. Tan, D. D. Johnson, Topologically correct phase boundaries and transition temperatures for Ising Hamiltonians via self-consistent coarse-grained cluster-lattice models, *Phys. Rev. B* 83 (2011) 144427.
- [5] K. G. Wilson, J. Kogut, The renormalization group and the  $\epsilon$  expansion, *Phys. Rep.* 12 (1974) 75–199.
- [6] J. Berges, N. Tetradis, C. Wetterich, Non-perturbative renormalization flow in quantum field theory and statistical physics, *Phys. Rep.* 363 (4) (2002) 223 – 386.
- [7] J. C. Le Guillou, J. Zinn-Justin, Critical exponents from field theory, *Phys. Rev. B* 21 (1980) 3976–3998.
- [8] A. Pelissetto, E. Vicari, Critical phenomena and renormalization-group theory, *Phys. Rep.* 368 (2002) 549–727.
- [9] C. Bagnuls, C. Bervillier, Exact renormalization group equations: an introductory review, *Physics Reports* 348 (1) (2001) 91–157, renormalization group theory in the new millennium. II. doi:[https://doi.org/10.1016/S0370-1573\(00\)00137-X](https://doi.org/10.1016/S0370-1573(00)00137-X).
- [10] T. Machado, N. Dupuis, From local to critical fluctuations in lattice models: A nonperturbative renormalization-group approach, *Phys. Rev. E* 82 (2010) 041128. doi:[10.1103/PhysRevE.82.041128](https://doi.org/10.1103/PhysRevE.82.041128).
- [11] A. Madsen, J. Als-Nielsen, J. Hallmann, T. Roth, W. Lu, Critical behavior of the order-disorder phase transition in  $\beta$ -brass investigated by x-ray scattering, *Phys. Rev. B* 94 (2016) 014111. doi:[10.1103/PhysRevB.94.014111](https://doi.org/10.1103/PhysRevB.94.014111).
- [12] R. J. Elliott, J. A. Krumhansl, P. L. Leath, The theory and properties of randomly disordered crystals and related physical systems, *Rev. Mod. Phys.* 46 (1974) 465–543.
- [13] V. I. Tokar, A new series expansion in lattice statistics, *Phys. Lett. A* 110 (1985) 453–456.
- [14] I. V. Masanskii, V. I. Tokar, Method of  $\gamma$ -expansions in the electronic theory of disordered alloys, *Theor. Math. Phys.* 76 (1) (1988) 747–757. doi:[10.1007/BF01029433](https://doi.org/10.1007/BF01029433).
- [15] C. Bervillier, Revisiting the local potential approximation of the exact renormalization group equation, *Nucl. Phys. B* 876 (2013) 587.

- [16] V. I. Tokar, A new renormalization scheme in the Landau-Ginzburg-Wilson model, *Phys. Lett. A* 104 (1984) 135–139.
- [17] V. I. Tokar, Calculation of non-universal thermodynamic quantities within self-consistent non-perturbative functional renormalization group approach (2019) arXiv:1904.10338.
- [18] S. Hori, An approach to a relativistic strong coupling theory, *Nucl. Phys.* 30 (1962) 644–663.
- [19] A. N. Vasiliev, *Functional Methods in Quantum Field Theory and Statistical Physics*, Gordon and Breach, Amsterdam, 1998.
- [20] E. Lieb, M. Loss, *Analysis*, CRM Proceedings & Lecture Notes, American Mathematical Society, Providence, RI, 2001.
- [21] J. F. Nicoll, T. S. Chang, H. E. Stanley, Exact and approximate differential renormalization-group generators, *Phys. Rev. A* 13 (1976) 1251–1264.
- [22] G. R. Golner, Nonperturbative renormalization-group calculations for continuum spin systems, *Phys. Rev. B* 33 (1986) 7863–7866. doi:10.1103/PhysRevB.33.7863.
- [23] Y. Ivanchenko, A. Lisyanskii, A. Filippov, New small rg parameter, *Physics Letters A* 150 (2) (1990) 100 – 104. doi:[https://doi.org/10.1016/0375-9601\(90\)90258-P](https://doi.org/10.1016/0375-9601(90)90258-P).
- [24] A. Parola, D. Pini, L. Reatto, First-order phase transitions, the Maxwell construction, and the momentum-space renormalization group, *Phys. Rev. E* 48 (1993) 3321–3332.
- [25] J.-M. Caillol, The non-perturbative renormalization group in the ordered phase, *Nuclear Physics B* 855 (2012) 854–884.
- [26] T. Morris, Equivalence of local potential approximations, *J. High Energy Phys.* 0507 (2005) 027.
- [27] R. J. Jelitto, The density of states of some simple excitations in solids, *J. Phys. Chem. Solids* 30 (3) (1969) 609–626.
- [28] H. J. Monkhorst, J. D. Pack, Special points for brillouin-zone integrations, *Phys. Rev. B* 13 (1976) 5188–5192.
- [29] V. Blum, A. Zunger, Mixed-basis cluster expansion for thermodynamics of bcc alloys, *Phys. Rev. B* 70 (2004) 055108.
- [30] I. V. Masanskii, V. I. Tokar, T. A. Grishchenko, Pair interactions in alloys evaluated from diffuse-scattering data, *Phys. Rev. B* 44 (1991) 4647–4649. doi:10.1103/PhysRevB.44.4647.

- [31] K. Radhakrishnan, A. C. Hindmarsh, Description and use of LSODE, the Livermore solver for ordinary differential equations, Tech. Rep. UCRL-ID-113855, LLNL (December 1993).
- [32] P. Lundow, K. Markström, A. Rosengren, The ising model for the bcc, fcc and diamond lattices: A comparison, *Phil. Mag.* 89 (22–24) (2009) 2009–2042. doi:10.1080/14786430802680512.
- [33] P. Butera, M. Comi, Extension to order  $\beta^{23}$  of the high-temperature expansions for the spin- $\frac{1}{2}$  ising model on simple cubic and body-centered cubic lattices, *Phys. Rev. B* 62 (2000) 14837–14843.
- [34] A. L. Talapov, H. W. J. Blöte, The magnetization of the 3d ising model, *J. Phys. A* 29 (1996) 5727.
- [35] A. J. Liu, M. E. Fisher, The three-dimensional ising model revisited numerically, *Physica* 156A (1989) 35–76.
- [36] C. Bagnuls, C. Bervillier, Nonasymptotic critical behavior from field theory at  $d = 3$ : The disordered-phase case, *Phys. Rev. B* 32 (1985) 7209–7231.
- [37] C. Bagnuls, C. Bervillier, D. I. Meiron, B. G. Nickel, Nonasymptotic critical behavior from field theory at  $d=3$ . II. The ordered-phase case, *Phys. Rev. B* 35 (1987) 3585–3607.
- [38] *Spherical volume element*, <https://en.wikipedia.org/wiki/N-sphere>.